CrystEngComm

Accepted Manuscript

ROYAL SOCIETY OF CHEMISTRY

www.rsc.org/crystengcomm

Journal Name

ARTICLE

Syntheses, crystal structures and properties of metal-organic rotaxane frameworks with cucurbit[6]uril

Received 00th January 20xx,
Accepted 00th January 20xx

DOI: 10.1039/x0xx00000x

www.rsc.org/

Jun Liang,[a,b] Xue-Song Wu,[a] Xin-Long Wang,[*a] Chao Qin,[a] Kui-Zhan Shao,[a] Zhong-Min Su,[*a] and Rong Cao[b]

Five new metal-organic rotaxane frameworks (MORFs) have been hydrothermally synthesized by systematically combining cucurbit[6]uril-based pseudorotaxanes, rigid carboxylate ligands and d^{10} metal ions. Compound **1** presents a three periodic pillared structure; **2** and **3** are two periodic layers with *hcb* topologies; **4** presents a 3D structure with *snw* topology and **5** is a three periodic network, featuring from interpenetrating to non-interpenetrating 3D MORF. The cucurbit[6]uril-based MORFs obtained in this work illustrate the importance of non-covalent interactions around CB[6]s in the assembly of resultant super architectures. Furthermore, their TGA analysis, solid photoluminescent properties and sensatization for lanthonide ions are investigated.

Introduction

The past decade has seen the tremendous efforts made by material chemists in exploiting coordinative bonds to create metal-organic framework (MOF) materials, which exhibit spectacular crystal structures and find potential applications in gas separation, catalysis, analytical chemistry, biomedicine and other applications.[1] Recently, the incorporation of mechanically interlocked molecules (MIMs),[2] such as catenanes, rotaxanes into crystalline polymers has demonstrated to be an effective way for a high level of molecular organization.[3] This is important as the majority of studies on MIMs focus mainly on their solution behavior where they are randomly dispersed and their motion is incoherent. So the combination of MIMs linkers and metal nodes via reticular synthesis has opened up a new avenue for the creation of a variety of novel functional matierals.[2c] As a subclass of these materials, metal-organic rotaxane frameworks (MORFs)[4] -in which macrocyclic molecule 'wheels' are threaded on the 'string' like linkers in one direction or another- continue to draw considerable interest since they could potentially lead to not just novel architectures but also prototypes of crystalline molecular machines. However, it is difficult to design and predict the final structures due to the enormous amount of non-covalent interactions involved in these systems. Thanks to the seminal work well performed by the Kim group, a series of cucurbit[6]uril-based pseudorotaxanes as linkers have been successfully incorporated in coordination polymers under mild conditions.[5] Then, Loeb and coworkers started their journey to fabricate another important family of MORFs containing crown ether and its derivatives.[6] As a result, several versions of MORFs have been obtained, including neutral ones.[6b] On the other hand, instead of using the predesigned pseudorotaxane or rotaxane linker strategy to obtain MORF, the Sessler group recently have exploited metal- or anion-directed self-assembly of organic macrocycles to get a set of MORFs containing the Texas-sized molecular box, in which anionic species are the threaded guests and linkers[7]. In addition, polyrotaxanes based on inorganic nanocluster "wheels",[8] cyclodextrin,[9a] or cyclobis(paraquat-p-phenylene),[9b] have also been reported. However, although many MORFs have been built with different macrocyclic molecules, it still remains an appealing challenge to construct high dimensional and functional MORFs with new topologies.[4b] The challenge lies in not only the design and laborious synthesis of active rotaxanes but also the reticular synthesis of targeted MORFs. It is believed that the key lies in the sensible choice of interlocked macrocycles and the synthesis strategy applied.[10]

Cucurbit[n]urils (CB[n]s), a family of rigid macrocyclic molecules with a hydrophobic cavity and two identical carbonyl fringed portals, have been extensively investigated in supramolecular chemistry,[11] and coordination chemistry[12]. The scientific insights derived from fundamental studies of cucurbit[n]uril and their analogues have been valuable in a wide range of applications, such as molecular switches, devices,[13] vesicles[14] and the development of ion channels, sensors and catalysis.[11b] Recent studies revealed that the "outer-surface interactions" of CB[n]s, such as π···π stacking,

[a] Institute of Functional Materials Chemistry, Key Laboratory of Polyoxometalate Science of Ministry of Education, Department of Chemistry, Northeast Normal University Changchun 130024, P. R. China Fax:+86 431 -85684009; E-mail: wangxl824@nenu.edu.cn; zmsu@nenu.edu.cn.
[b] Department of Chemistry, College of Chemistry and Chemical Engineering, Xiamen University Xiamen 361005， P. R. China

† Electronic Supplementary Information (ESI) available: PXRD, TGA, FL, UV, crystallographic data, post-synthetic modification processes. See DOI: 10.1039/x0xx00000x

hydrogen bonding and C–H···π interactions, could have significant effect on the formation of some remarkable architectures and inorganic-organic hybrid materials.[15] Despite that some MORFs containing rigid CB[6]-based pseudorotaxanes have been obtained, the employment of flexible CB[6]-based supramolecular linkers for the self-assembly of MORFs has less been investigated, perhaps due to the dynamic nature of these pseudorotaxane building blocks.[16] Considering the powerful strategy of using mixed ligands for fabricating the variety of functional solid state materials (SSMs),[17] we noticed that little progress has been made in exploiting this strategy for exploring new MORFs.[3d,18]

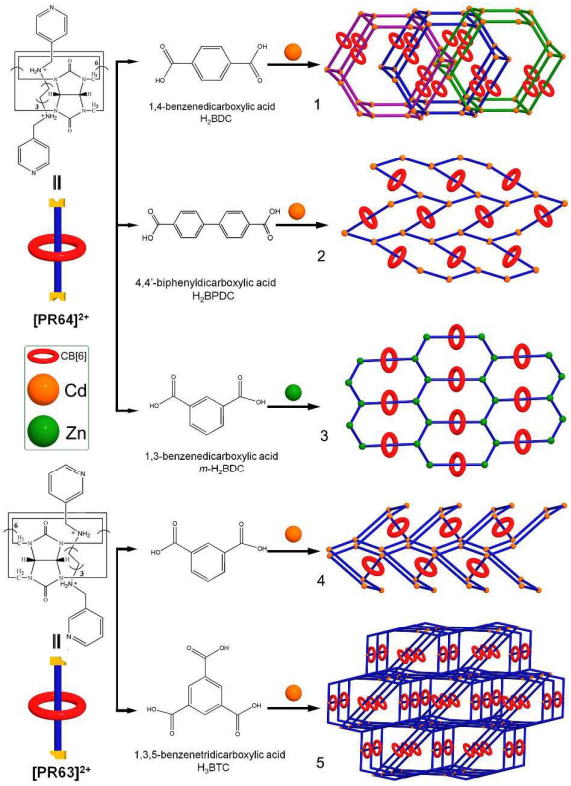

Scheme 1. Synthesis and schematic views of the 3D pillared-layer structure in **1**; the 2D wavy layer in **2**; the 2D flat (6, 3) net in **3**; the 3D branched MORF-**4** and the (3, 3, 4, 4)-connected network in **5**. Sticks without cucurbit[6]uril wheels represent unit with terminal carboxylic acid groups.

Herein, we investigate the coordination-driven self-assembly of two CB[6]-based pseudorotaxanes {$[PR6n]^{2+}\cdot 2[NO_3]^-$, n=3, 4},[19] four rigid geometry varied carboxylate ligands *p*-phthalic acid (H_2BDC), 1,3-Benzenedicarboxylic acid (*m*-H_2BDC), 1, 3, 5-Benzenetricarboxylic acid (H_3BTC) and 4, 4'-biphenyldicarboxylic acid (H_2BPDC) and d^{10} metal ions, and report five novel MORFs (Scheme 1 and Fig. S1†). Our investigations were aimed at constructing new cucurbit[6]uril-based MORFs crystalline materials and discussing the synergetic effect of different linkers on the final architectures. The main difference between pseudorotaxanes {$[PR6n]^{2+}\cdot 2[NO_3]^-$, n=3, 4} lies in their different terminal coordination groups, which may endow them with different behaviours during the self-assembly process. In addition, the preparation of photoluminescent composites **3:Ln** (Ln = Sm^{3+}, Eu^{3+}, $Tb^{3+}$and Dy^{3+}) indicated that **3** had the potential for sensitizing visible emitting lanthanide cations on the surfaces as demonstrated by FL, PXRD and ICP(†). It should be noted that, up to now, the post-synthetic modification (PSM) of MOFs containing uncoordinated carbonyl groups has relatively less been reported.[20] This work may provide new opportunities for MOFs with functional macrocyclic molecules,[21] including cyclodextrins (CDs), calix[n]arenes, pillar[n]arenes.

Experimental

General procedures

$[PR63]^{2+}\cdot 2[NO_3]^-$, $[PR64]^{2+}\cdot 2[NO_3]^-$ and CB[6] were synthesized according to references.[19] Other purchased chemicals (analytical pure) were used without further purification except *m*-H_2BDC and H_2BPDC, which were prepared as their sodium salts by NaOH before use in certain cases. The formulae of all compounds were obtained by single-crystal X-ray diffraction, thermogravimetric analysis (TGA) and by taking into account charge balance considerations. The IR spectra were recorded from KBr pellets in the range of 4000–400 cm^{-1} on a Mattson Alpha-Centauri spectrometer. Elemental analyses (C, H, and N) were performed on a Perkin-Elmer 2400 elemental analyzer. Thermogravimetric analysis (TGA) was performed on a Perkin-Elmer TG-7 analyzer over the temperature 50–700 °C in a nitrogen-gas atmosphere with a heating rate of 10 °C min^{-1}. Solid-state luminescent spectra were measured on a Cary Eclipse spectrofluorometer (Varian) equipped with a xenon lamp and quartz carrier at room temperature. Inductively coupled plasma (ICP) was measured by ICP-9000(N+M) (USA Thermo Jarrell-Ash Corp). UV-Vis absorption spectra were obtained using a 752 PC UV-Vis spectrophotometer. Powder XRD measurements were recorded on a Siemens D5005 diffractometer with Cu-Kα (λ = 1.5418 Å) radiation in the range 3–50°.

X-ray Diffraction analysis

Single-crystal X-ray diffraction data for compound **1**-**5** were recorded on a Bruker Apex CCD II area-detector diffractometer with graphitemonochromated Mo-Kα radiation (λ = 0.71073 Å) at 298(2) K. Absorption corrections were applied using multi-scan technique and performed by using the SADABS program. The structures of all compounds were solved by direct methods and refined on F^2 by full-matrix least squares methods using the SHELXTL package. Figures were drawn with DIAMOND software.[22b] CCDC-1052456 (**1**), 1052457 (**2**), 1052459 (**3**), 1052460 (**4**) and 1052461 (**5**) contain the supplementary crystallographic data for this paper. These data can be obtained free of charge from The Cambridge Crystallographic Data Centre via *www.ccdc.cam.ac.uk/data_request/cif*. Anisotropic thermal parameters were used to refine all non-hydrogen atoms except for part of oxygen and carbon atoms when NPD

problems could occur for these atoms. Hydrogen atoms on carboxylate ligand were placed on calculated positions and included in the refinement riding on their respective parent atoms. In compound **1**, **2** and **3**, the $[PR64]^{2+}$ cation lies about an inversion center. In **1**, atoms C20 and C21 of the axle's chains are disordered over two positions (50/50). In **2**, the axle unit and the cucurbit[6]uril molecule can be completed via the (-x, 1-y, -z) symmetrical operation. While the coordination sphere of Cd can be completed through the (1+x, 1.5-y, -0.5+z) operation. In **3**, the axle unit and the cucurbit[6]uril molecule can be completed via two independent symmetrical operations (-x, 2-y, -1-z; -x, 1-y, -2-z). Atoms C16 and C17 of the axle's unit are disordered over two positions (50/50 and 60/40, respectively). In the tetragonal compound **4**, the $[PR63]^{2+}$ cation lies about a twofold axis. In compound **5**, the two independent half axles cations can be completed via the two independent symmetrical operations (1-x, -y, -1-z; 2-x, -1-y, -z). Atoms C26, C27, C35 and C36 of the axles' units are disordered over two positions (50/50). While the two independent half cucurbit[6]urils could be completed via two independent symmetrical operations (-x, 1-y, -z; 1-x, -y, 1-z).

Synthesis of 1. $[Cd_2(BDC)_3(PR64)]\cdot 9H_2O$: A mixture of $[PR64]^{2+}\cdot 2[NO_3]^-$ (82 mg, 0.05 mmol), $CdSO_4\cdot 8H_2O$ (230 mg, 0.3 mmol), H_2BDC (0.2 mmol, 33 mg), triethylamine (2 drops, where 1ml injection syringe is used) in water (3.5 ml) was heated at 140°C for 48 h in a Teflon-lined stainless steel container and cooled to room temperature. Block colorless X-ray-quality crystals were collected and dried in air (yield: 20% based on $[PR64]^{2+}.2[NO_3]^-$). Elemental analysis calc. for $C_{78}H_{106}N_{28}O_{39}Cd_2$ (%): C, 41.01; N, 17.17; H, 4.68; Cd, 9.84; Found: C, 41.53; N, 17.67; H, 4.24; Cd, 9.95. IR (cm^{-1}, major absorbances): 3444 (w), 1733 (s), 1566 (s), 1474 (s), 1377 (w), 1234 (s), 1189 (s), 963 (s), 800 (m).

Synthesis of 2. $[Cd(BPDC)(PR64)_{0.5}Cl]\cdot 2H_2O$: A mixture of $[PR64]^{2+}\cdot 2[NO_3]^-$ (82 mg, 0.05 mmol), $CdCl_2\cdot 2.5H_2O$ (69 mg, 0.3 mmol) and H_2BPDC (0.1 mmol, 24.2 mg) in 5 ml water/dimethyl formamide (4:1(v)) was sealed in a Teflon-lined stainless steel container, which was heated at 120°C for 48 h, and cooled to room temperature. Flaky colorless X-ray-quality crystals were collected (yield: 26% based on $[PR64]^{2+}.2[NO_3]^-$). Elemental analysis calc. for $C_{41}H_{46}N_{14}O_{13}CdCl$ (%): C, 45.15; N, 17.98; H, 4.25; Cd, 10.31; Found (%): C, 45.28; N, 18.53; H, 4.02; Cd 10.05. IR (cm^{-1}, major absorbances): 3504 (w), 1735 (s), 2991 (w), 2933 (w), 1673 (s), 1473 (s), 1396 (m), 1237 (s), 1188 (s), 966 (s), 800 (m).

Synthesis of 3. $[Zn(PR64)_{0.5}(m\text{-}BDC)Cl]\cdot 3H_2O$: A mixture of $[PR64]^{2+}\cdot 2[NO_3]^-$ (82 mg, 0.05 mmol), $ZnCl_2$ (13.6 mg, 0.1 mmol), *m*- Na_2BDC (0.1mmol, 21mg) in water (5 ml) was sealed in a Teflon-lined stainless steel container, which was heated at 120°C for 48 h, and cooled to room temperature. Fine block colorless X-ray-quality crystals were collected and dried in air (yield: 31% based on $[PR64]^{2+}.2[NO_3]^-$). Elemental analysis calc. for $C_{35}H_{40}N_{14}O_{13}ZnCl$ (%): C, 43.53; N, 20.31; H, 4.18; Zn, 6.77; Cl, 3.67; Found (%): C, 43.27; N. 20.46; H, 4.04; Zn, 6.63. IR (cm^{-1}, major absorbances): 3535 (w), 1741(w), 1630 (w), 1474 (s), 1379 (w), 1189 (s), 965 (m), 799 cm^{-1} (m).

Synthesis of 4. $[Cd_{1.5}(m\text{-}BDC)_2(PR63)_{0.5}(H_2O)_2]\cdot 7H_2O$: A mixture of $[PR63]^{2+}\cdot 2[NO_3]^-$ (82 mg, 0.05 mmol), $Cd(NO_3)_2\cdot 4H_2O$ (61.6 mg, 0.2 mmol), *m*-H_2BDC (33mg, 0.2mmol), triethylamine (3 drops) in 3.5 ml of water was kept at 140°C for 48 h in a Teflon-lined stainless steel container and cooled to room temperature. Polyhedral light yellow crystals were collected and dried in air (yield: 35% based on $[PR63]^{2+}.2[NO_3]^-$). When $CdSO_4\cdot 8H_2O$ was used, higher production of compound **4** could be obtained. Elemental analysis calc. for $C_{86}H_{122}N_{28}O_{49}Cd_3$ (%): C, 38.70; N, 14.69; H, 4.61; Cd, 12.63; Found (%): C, 38.58; N, 14.26; H, 4.36; Cd, 12.75. IR (cm^{-1}, major absorbances): 3434 (w), 1738 (s), 1604 (s), 1472 (s), 1379 (w), 964 (s), 800 cm^{-1} (s).

Synthesis of 5. $[Cd_{2.5}(BTC)_2(PR63)(NO_3^-)(H_2O)_3]\cdot 8H_2O$: A mixture of $[PR63]^{2+}\cdot 2[NO_3]^-$ (82 mg, 0.05 mmol), $Cd(NO_3)_2\cdot 4H_2O$ (123.4 mg, 0.4 mmol), H_3BTC (21.0 mg, 0.1 mmol), triethylamine (8 drops, where 1ml injection syringe is used) in water (3.5 ml) was heated at 140°C for 48 h in a Teflon-lined stainless steel container. The resulted small flaky colorless X-ray-quality crystals were collected by manual and dried in air (yield: 18% based on $[PR63]^{2+}.2[NO_3]^-$). Elemental analysis calc. for $C_{144}H_{164}N_{58}O_{72}Cd_5$ (%): C, 39.12; N, 18.37; H, 3.74; Cd. 12.71; Found (%): C, 38.89; N. 18.14; H, 4.05; Cd. 12.48. IR (cm^{-1}, major absorbances): 3441 (w), 1737 (s), 1614 (s), 1557 (s), 1472 (s), 1374 (s), 1234(s), 1188 (s), 964 (s), 801 cm^{-1} (s).

Results and discussion

Crystal structures of compounds 1-5

The reaction of $[PR64]^{2+}\cdot 2[NO_3]^-$ with H_2BDC and $CdSO_4$ under hydrothermal conditions gave X-ray quality crystals of **1** $[Cd_2(BDC)_3(PR64)]\cdot 9H_2O$ with a neutral pillar-layer MORFs. **1** crystalized in the monoclinic, space group C2/c and the asymmetric unit contains one independent Cd^{2+} ions, one and a half BDC^{2-} anions, half a $[PR64]^{2+}$ and several water molecules. The Cd metal center is coordinated by five oxygen atoms from three separate BDC^{2-} ligands in a bidentate mode (Cd-O: 2.226-2.441 Å), and one N atom from $[PR64]^{2+}$ connector (Cd-N: 2.299 Å) with a pentagonal pyramidal geometry (Fig. 1a). Topological analysis using TOPOS program identifies the propagated single 3D net as *sra* topology with the point symbol of ($4^2.6^3.8$) (Fig. 2d). [22]

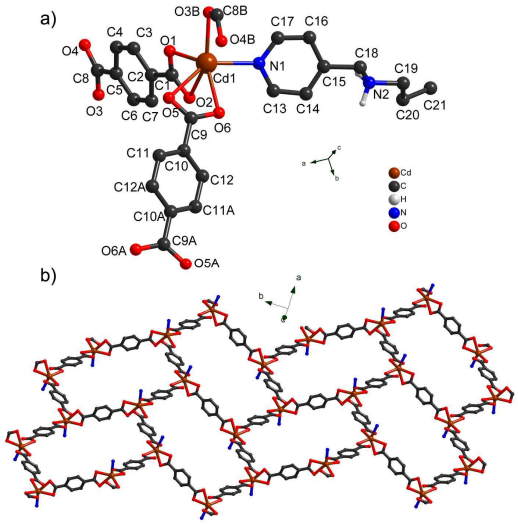

Fig. 1. a) Ball-and-stick representation of the asymmetric unit of **1**. Hydrogen atoms and CB[6]s are omitted for clear. Symmetry codes: A: 1.5-x, 0.5-y, 1-z; B: x, -y, 0.5+z; b) The 2D wavy layer in **1**.

Firstly, a wavy 2D layer with honeycomb pores (average bidiagonal Cd-Cd distance: 22.156 Å) is formed by BDC^{2-} and Cd centers acting as a 3-connected node (Fig. 1b). Then the adjacent layers are further connected by the 2-connected [PR64] ligands and this propagates into the overall 3D pillared architecture, with an approximate distance of 20.75 Å between adjacent layers (Fig. 2a and 2b). For each of the [PR64] ligands (green⊂orange), although the protonated alkylamines axle takes *trans*-configuration, two terminal pyridine groups are not in parallel, with the dihedral angles of 52.24°. This is accompanied by the π···π interactions (3.610 Å) in $[PR64]^{2+}$, which makes it robust as a pillar linker (Fig. S2 and S3a†). Furthermore, the large openings of dumbbell-shaped void space in this 3D metal–organic rotaxane framework allows other two identical frameworks to interpenetrate the first one, regardless of the bulky CB[6]s (Fig. 2c). Calculations using PLATON show that the effective pore volume for **1** is only 5.1% (525.2 $Å^3$) per unit cell (10200 $Å^3$), which is occupied by water molecules.[22c] Fig. 2e illustrates a scheme presentation of the whole 3-fold interpenetrated *sra* nets with the 'bead' on each pillar rod. Up to now, only a few 3D MORFs containing CB[6] have been obtained.[5d,5g,5j] Here, **1** represents a three-dimensional CB[6]-based MORFs where pseudorotaxanes are used as pillar ligands.[3d] Interestingly, $[PR64]^{2+}$ might have played a template role through C-H···π (2.73 Å) as well as weak π···π interactions (3.71 Å) in **1**, as all CB[6]s in one net are well arrayed between two wavy layers from other interpenetrated nets (Fig. S3c†). A more interesting feature in **1** could be the observation of an inseparate hybrid molecular necklaces HMN[5] as well as a novel 1D 'polycatenanes' just derived from the catenation of rings via Hopf links, with two additional CB[6] beads on each ring units.[23] (Fig. S4†). So **1** shows the characteristics of molecular necklaces, polyrotaxanes and polycatenanes.

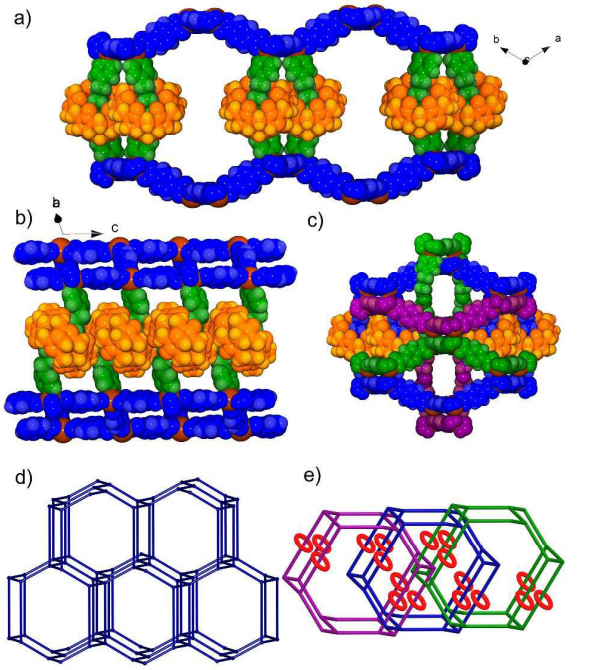

Fig. 2. a) and b) Different perspectives of the single pillared-layer framework of **1** in space-filling mode. c) One framework (blue) interpenetrated by other two identical frameworks (violet and green). CB[6]s (orange) are shown only in one net. d) View of the *sra* topology of MORF-**1**. e) A scheme presentation of the 3-fold interpenetrating 3D architectures in **1**.

Encouraged by the above system, the Cd^{2+} directed assembly of $[PR64]^{2+}\cdot 2[NO_3]^-$, H_2BPDC has led to single crystals of **2** $[Cd(BPDC)(PR64)_{0.5}Cl]\cdot 2H_2O$ with 2D wavy layers (Fig. 3a). The basic hexa-nuclear cadmium-organic loop in each net can be easily observed and it is formed by six Cd ions, four $BPDC^{2-}$ anions, two $[PR64]^{2+}$ ligands and six chloride atoms. Each Cd center is coordinated in a distorted octahedral mode by four oxygen atoms from two separate BPDC ligands in a bidentate mode (Cd-O: 2.29-2.46 Å), one N atom from $[PR64]^{2+}$ connector (Cd-N: 2.348 Å) and one coordinated chloride ion (Cd-Cl: 2.482 Å). Compared with the $[PR64]^{2+}$ in **1**, two terminal pyridine groups in each *trans*-$[PR64]^{2+}$ are in parallel. It is worth noting that, although all CB[6]s in any specific layer are in the same plane, the framework is so wavy that it takes other three layers to offset the gap with a height of 21.84 Å and dihedral angle of 62.5°(Fig. 3b and 3c). Deeper analysis on the non-covalent interactions around $[PR64]^{2+}$ reveals that the alternating layers are staggered in a tiling array manner via π ···π stacking interactions (3.69 Å) involving CB[6]s and $BPDC^{2-}$ (Fig. S5†). As a result, all CB[6]s of adjacent frameworks are well separated and arrayed in a line along the *a* axis. This packing pattern of CB[6]s in **2** is reminiscent of hexagonal CB[6] *P6/mmm* crystals with perfectly aligned one dimensional macrocycle nanotubes, but the latter isn't stable in air.[27c] PLATON show that the effective pore volume for **2** is about 8.2% (390.9 $Å^3$) per unit cell (4762.0 $Å^3$), which is also occupied by water molecules. What shouldn't be ignored is that each $BPDC^{2-}$ is curved by a torsional twist of 50.70° with respect to

their contiguous aromatic rings, partially due to the hydrogen bonds around it (Fig. S6†). The structures of **1**-**2** demonstrated that the ligand length could lead to different architectures.

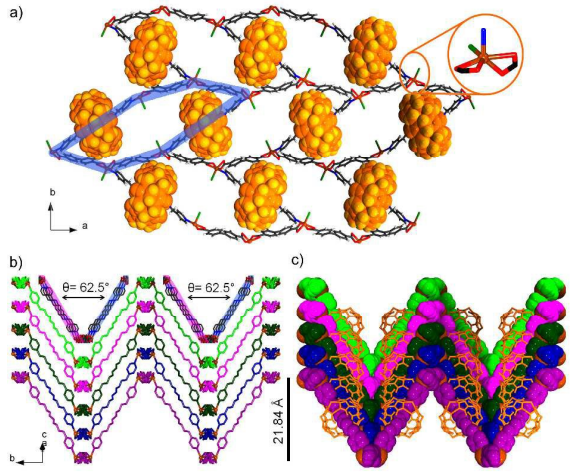

Fig. 3. a) A single layer of **2** as viewed along the *c* axis. The stick and space-filling views of five stacked wavy layers b) without and c) with CB[6]s. Individual layers are marked in different colors. Color code: black: C; blue: N; red: O; green: Cl; gray: H; orange: CB[6]. Inset : Cd node.

These intriguing architectures obtained above promoted us to extend auxiliary ligands, such as *m*-H_2BDC and H_3BTC. Firstly, the combination of $[PR64]^{2+}\cdot 2[NO_3]^-$, *m*-$H_2$BDC and $ZnCl_2$ leads to a two dimensional flat layer of **3** $[Zn(PR64)_{0.5}(m\text{-}BDC)Cl]\cdot 3H_2O$, as shown in Fig. 4a. Each Zn center is coordinated in tetrahedral mode by two oxygen atoms (Zn-O: 1.930-1.943 Å) from two *m*-BDC^{2-} ligands, one N atom (Zn-N: 2.065 Å) from *trans*-$[PR64]^{2+}$ connector and one coordinated chloride atom (Zn-Cl: 2.251 Å). This structure is similar to that of 2D crown ether-based polyrotaxane, which is only one of the directions employs the rotaxane linker.[4a] It also has the same *hcb* topology as that of **2**. While **3** contains oblate hexagon rings (bidiagonal Zn-Zn mean distance: 28.937 Å), largely due to the given configuration of *m*-BDC as well as the tetramer unit of CB[6]s formed by C–H···π (average 2.78 Å) and π···π interactions (3.34-3.50 Å) between CB[6]s of one hexagon ring and two CB[6]s from adjacent two layers (Fig. S7†). And it's the cumulative effect of these non-covalent bonding interactions that leads to a 3D supramolecular structure, in which adjacent layers are closely stacked in an inlaid manner (Fig. 4b).

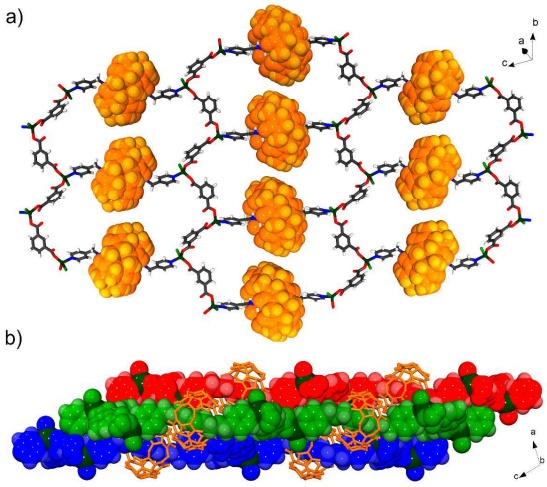

Fig. 4. a) The chemical view of 2D layer in **3**, the individual CB[6] components in space-filling mode. b) The stacking view of adjacent layers in an inlaid manner. Color code: black: C; blue: N; red: O; green: Cl; dark green: Zn; gray: H; orange: CB[6].

When $[PR63]^{2+}\cdot 2[NO_3]^-$ and *m*-H_2BDC ligands were harnessed to coordinate with Cd^{2+} ions, the 3D branched architecture of **4** $[Cd_{1.5}(m\text{-}BDC)_2(PR63)_{0.5}(H_2O)_2]\cdot 7H_2O$ was readily obtained.

As shown in Fig. 5a, there are one and a half crystallographically independent Cd^{2+} atoms (Cd1 and Cd2), two *m*-BDC^{2-} anions, half a $[PR63]^{2+}$ and two coordinated water molecules in the asymmetric unit of **4**. Cd1 is seven-coordinated by six oxygen atoms from three separate *m*-BDC ligands and one nitrogen atom from $[PR63]^{2+}$. While Cd2 is coordinated in an octahedral fashion by two oxygen atoms from two separate *m*-BDC^{2-} ligands and four coordinated water molecules. The bond lengths of Cd–O (2.232–2.552 Å) and Cd–N (2.327 Å) are close to the reported compounds. The adjacent Cd1 atoms are connected by $[PR63]^{2+}$ and *m*-BDC^{2-} ligands with Cd1-Cd1 distances: 11.452, 10.098, 17.116 Å, respectively, forming a 3D *snw* network with the point symbol of $(6^3.8^3)$ (Fig. S8c†).[24] It is noted that the diaminoalkanes axle of *cis*-$[PR63]^{2+}$ here is rather curved (13.64 Å based on centroid distance of two terminal pyridine groups) when coordinating with metal ions (Fig. 5) and this was not discovered before.[19] It is mainly due to the twisting of the hexylidene in the "string" and being stabled by strong coordination interactions as well as by the π···π stacking effect between *m*-BDC^{2-} and rings of CB[6] in $[PR63]^{2+}$ (Fig. S3d†).

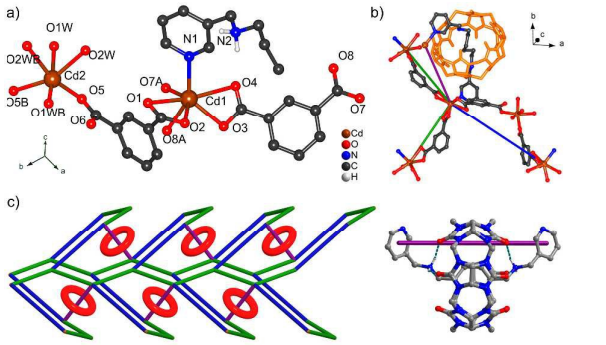

Fig. 5. Ball-and-stick representation of a) the asymmetric unit of **4**. CB[6] was omitted; b) the simplified repeated unit composed of *m*-BDC^{2-} $[Cd(m\text{-}BDC^{2-})_2{\cdot}4Ow]$ and $[PR63]^{2+}$ units in **4**; c) A catoon depiction of the 3D branched MORFs in **4**. Color code: green: *m*-BDC; blue: $[Cd(m\text{-}BDC^{2-})_2{\cdot}4Ow]$; violet rod: $[PR63]^{2+}$; orange or red: CB[6]. Symmetry codes: A (1.5-x, 0.5+y, 1.25-z); B (1+x, -1+y, 1-z).

To understand the 3D branched MORFs fully, we shall start from the chemical environment of CB[6]s. First of all, one 1 D elliptic cylindrical MORF was formed along the *b* axis with two lines of intrinsic CB[6]s (9.1 Å height) well arranged in this indefinite tunnel with a parameter of approximate 9.3×36.3 Å (Fig. S8a†). Then these curved 1D tunnels propagated into a 2-periodic thick sheet with wavy surfaces by shearing the relatively flat surfaces along the *a* axis (Fig. S8b†). After that, the resulted 2D MORFs extended itself along the *c* axis by shearing wavy surfaces, which eventually lead to a 3D *snw* MORFs (Fig. S8c†). Due to the special arranged way, a beautiful branched polyrotaxanes could be easily distinguished (Fig. 5c). This special architecture makes us reminiscent of pseudorotaxane-terminated dendrimers containing CB[6]s reported by Kim[25a] and crown ethers-based supramolecular metallodendrimers by Yang,[25b] but here CB[6] beads are dispersed in a highly ordered manner in an indefinite 3D crystal lattice.

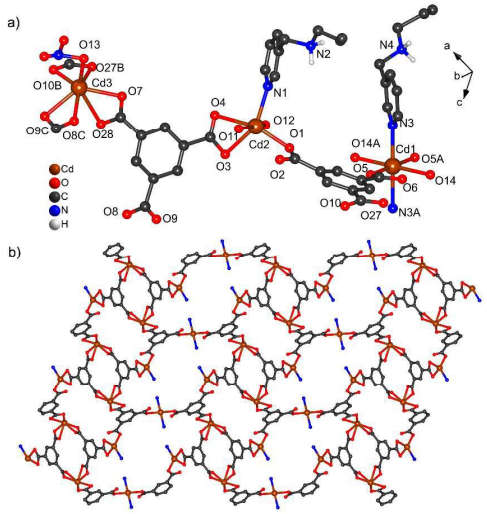

Fig. 6. a) The coordination environment of Cd atoms in **5**. CB[6] was omitted. Symmetry codes: A (1-x, -y, -z); B (1+x, 1+y, z); C (3-x, 1-y, 1-z). b) Chemical view of the 2D wavy layer.

When $[PR63]^{2+}{\cdot}2[NO_3]^-$, H_3BTC ligand were coordinated with Cd^{2+} ions, a new high dimensional structure of **5** $[Cd_{2.5}(BTC)_2(PR63)(NO_3^-)(H_2O)_3]{\cdot}8H_2O$ was obtained. The asymmetric unit of **5** contains two BTC^{3-} anions, two and a half independent Cd^{2+} ions, one $[PR63]^{2+}$, one coordinated nitrate ion and three coordinated water molecules. The bond lengths of Cd–O (2.156–2.527 Å) and Cd–N (2.266-2.30 Å) are close to the reported compounds.

As shown in Fig. 6a, the adjacent Cd atoms are linked by BTC^{3-} ligands, forming a 2-periodic wavy layer containing three ring species, including 16-, 32- and 48-membered rings (Fig. 6b). If the 16-membered rings can be viewed as 4-connected nodes, linked with two BTC^{3-} anions and coordinated by two Cd ions, and BTC^{3-} beyond that rings as 3-connected linkers, a simple 3,4-connected layer was observed first (Fig. S9†). Finally, these 2-periodic wavy layers are linked by α-$[PR63]^{2+}$ to furnish a three dimensional 3, 3, 4-c pillar-layer MORF with a distance of 19.344 Å between adjacent layers (Fig. 7a and Fig. S9†). Then the spacious openings of this framework allow another identical framework to 'interpenetrate' it, which is like that found in compound **1** in so far as interpenetration happens (Fig. 7b). But here, the void space left by the resulted virtual '2-fold interpenetrating frameworks' is properly large enough to accommodate another kind of pseudorotaxanes (β-$[PR63]^{2+}$), which effectively merge these two identical nets into one novel three dimensional MORF through coordinating with Cd2 node (Fig. 7c and Fig. S10†). PLATON calculations reveal that the effective pore volume for **5** is only about 5.8% (263.5 $Å^3$) per unit cell (4540.0 $Å^3$), which is also occupied by water molecules.[22c] Fig. 8d illustrates the whole non-interpenetrating network constructed from four of the building blocks. The whole framework is a new 3, 3, 4, 4-c net with the point symbol of $(10^6)(6.10^2)_2(6.8^2)_2(6^2.8^2.10^2)$. Topological classification with the TOPOS TTD collection reveals that such a net has never been found in coordination polymers.

Furthermore, the α-$[PR63]^{2+}$ played a 'template' role in this structure as the 48-membered rings are formed around it and there exist two-fold weak π···π interactions (3.68 Å and 3.90 Å) between pyridine moieties (Fig. S11†). And so does β-$[PR63]^{2+}$ by weak π···π interactions (3.628-3.750 Å) around CB[6]s. In addition, there are π···π interactions (3.271 Å) in β-$[PR63]^{2+}$, which makes it more rigid and shorter than α-$[PR63]^{2+}$, as a result (Fig. S11c†). The structures of **4** and **5** revealed not only that geometry varied assisted ligands could lead to different frameworks, but that $[PR63]^{2+}$ seemed to be conformationally more flexible than $[PR64]^{2+}$.

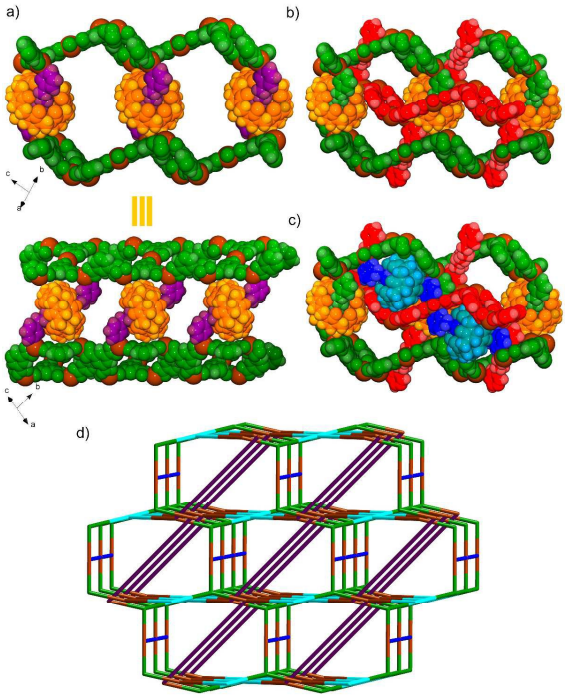

Fig. 7. The space-filling representations of the virtual a) single and b) twofold interpenetrating pillared-layer structure in **5**. c) Same view showing two identical frameworks merged into one framework by *θ*-$[PR63]^{2+}$. d) A schematic of topology framework of **5**. Color code: violet or blue: $[PR63]^{2+}$; green: BTC ligands; cyan: 16-membered rings; brown: Cd ions.

To get the characteristics of $[PR64]^{2+}$ and $[PR63]^{2+}$ in detail in these compounds, we define two structural parameters, *d* and *δ* (Table S2†). Both the length (*d*) and the dihedral angles (*δ*) between two terminal pyridine groups in $[PR64]^{2+}$ and $[PR63]^{2+}$ could vary obviously in specific reaction systems. The results of the calculated *d* and *δ* values for pseudorotaxane in **1**-**5**, together with that of the previously reported $[PR64]^{2+}$ or $[PR63]^{2+}$ containing compounds[19] are tabulated in Table S2†. It can be seen that the combination of flexibility in the protonated alkylamines axis and rigidity of CB[6] in $[PR64]^{2+}.2[NO_3]^-$ and $[PR63]^{2+}.2[NO_3]^-$ renders them as rather flexible linkers to construct multi-dimensional MORFs. We suggest that the configuration of these pseudorotaxanes could be largely affected by their chemical environment during the assembly process, but it is quite difficult to predict the final architectures when assisted carboxylic ligands are introduced, which is different from the situation for constructing 1D polyrotaxanes.[19] However, the incorporation of aromatic anionic ligands could effectively eliminate the unnecessary counter ions in the resultant MORFs as indicated in work herein.[4b]

Powder X-ray diffractions (PXRD) and thermogravimetric analyses (TGA)

The phase purity and homogeneity of all products was confirmed by the well agreement between the experimental X-ray powder diffraction (XRPD) patterns and the simulated patterns based on structure analysis (Fig. S17-S21†). TGA were performed from 50 to 700 ℃ to investigate the thermal stability of compounds **1**, **2**, **3**-**5** as well as the determination of water molecules present in each compound. The TGA curves of compound **1** (Fig. S22†) exhibited continuous weight losses between 50 and 260 ℃, corresponding to the release of free and coordinated water molecules (9 water molecules for **1**, calc. 7.08%; found: 7.09 %). The following further weight losses (in the range from 260 to 700 ℃) is attributable to the decomposition of the organic components in **1**. Compounds **2**, **3–5** (Fig.S22 and S23†) showed the first step of weight losses before 300 ℃, which corresponded to the loss of water molecules (2 water molecules for **2**, calc. 3.30%; found: 4.17 %; 3 water molecules for **3**, calc. 5.58%; found: 5.00 %; 11 water molecules for **4**, calc. 7.42 %; found: 9.47 %; 11 water molecules for **5**, calc.4.48 %; found: 8.1 %). Compared with compounds **1**, further rapid weight losses of compounds **2**, **3–5** could be observed at higher temperatures (around 330 ℃ for **4** and **5**, 360 ℃ for **2**, 370 ℃ for **3**) due to the decomposition of organic components. The thermal stability of **3** was studied by PXRD at different temperatures and the result showed that **3** could be stable up to 370 ℃ which agrees with the TG curve (Fig. S24†). The good thermal stability of **3** might be explained by the unique inlaid arrangement of adjacent layers driven by the abundant hydrogen interactions and π···π interactions (Fig. S7†).

Fluorescence of compound 1, 2, 3, 4 and 5

The solid-state photoluminescent spectra of organic linkers and compound **1**-**5** at room temperature were investigated (Fig. S25†). The wavelengths of the emission maxima and excitation are listed in the Table S3†. The photoluminescence emission spectra of **1**-**5** have broadband peaks with maxima at 429, 410, 383, 494 and 412 nm, under certain excitation maximum respectively (Fig. S25†). Compared with that of related carboxylate ligands, emission spectra of **1** and **5** are slightly red-shifted (42 and 25 nm, respectively), which may be ascribed to the intra-ligand emission and the intermolecular interactions (such as π···π stacking) between the molecules in the solid state.[26] This also explained the broad band emission of **3** at around 383 nm (λ_{ex}= 312 nm), due to intra-ligand (π–π* and n-π*) fluorescent emission.[26b] The emission spectra of **2** is almost the same with that of H_2BPDC (λ_{em}= 408), which might be just due to the intra-ligand (n–π*) emission. While **4** shows a broad emission peak between 400 nm and 650 nm with the emission maximum at 494 nm. The strong fluorescence emission and distinct red-shift (114 nm) may be ascribed to the intra-ligand emission and ligand-to-metal charge transfer (LMCT).[26d]

Photoluminescence of composites 3:Ln (Ln= Sm^{3+}, Eu^{3+}, Tb^{3+}, Dy^{3+})

Considering the enormous amount of carbonyl groups on the surfaces of these crystals, we tried to investigate the sensitization ability of MORFs toward visible emitting lanthanide cations.[20,27] PXRD patterns collected for **X:Eu** (X=**1**, **3**, **4**, **5**) showed that the solid samples maintained their full crystallinity (Fig. S17-S21†). Fig. 8 shows the photographs of these composites excited by a standard laboratory ultraviolet lamp (254 nm), which indicated that the **1:Eu** and **3:Eu**, as

better emitters than **4:Eu** and **5:Eu** (pink colour), emitted a distinctive red colour, which was readily observed by the naked eyes as a qualitative indication of europium sensitization. In contrast, **CB[6]HP:Eu** and europium nitrate showed no noticeable emitting under the same conditions.

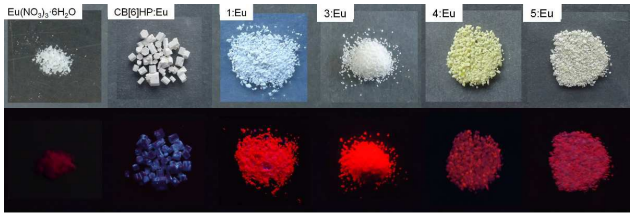

Fig. 8. Samples illuminated with daylight (top) and a 254 nm laboratory UV light (bottom). From left to right: $Eu(NO_3)\cdot 6H_2O$ and **X:Eu** (X = **CB[6]HP**, **1**, **3**, **4**, **5**).

The photoluminescence performance on each composite of **X:Eu** (X=**1**, **3**, **4**, **5**, **CB[6]HP**) and corresponding compounds were compared. As shown in the Fig. S26-S29†, compared to the photoluminescence excitation (PLE) spectra of original compound **n** (n= **1**, **3**, **4, 5**), a new enhanced broad excitation band around 280 nm is observed for **X:Eu** (X=**1**, **3**, **4**, **5**), which may be likely attributable to the adsorption of aromatic carboxylic ligands.[27] The typical $^7F_0 \rightarrow {}^5L_6$ transition peaks of Eu^{3+} could also be observed in these composites to some extent, but they were apparently much weaker than that of ligands, which indicated the energy transfer from the ligand to the metal ions, especially for composite **3:Eu**. Specifically, Eu^{3+} ions could have coordinated effectively with carboxylic groups on the crystal surfaces.[26b] In contrast, the PLE spectra of **CB[6]HP:Eu** indicated that solid CB[6] crystals showed negligible sensing ability for Eu^{3+} ions under identical condition (Fig. S30†). ICP data showed that the amount (wt%) of Eu^{3+} ions on the surfaces of **X:Eu** (X=**1**, **3**, **4**, **5)** were 2.1, 4.16, 2.15, 1.29, respectively (Table S4†). The different amount of visible emitting ions on corresponding crystals may be related to their different structures. Note that all CB[6]s are well dispersed in the frameworks of **1** and **3** in almost one direction (Fig. S12-S13†). Nevertheless, CB[6]s are highly entangled in the frameworks of **4** and **5**, being arranged in multi-directions (Fig. S14-S15†). As for CB[6] crystals, it is well known for the self-closing effect, in which CB[6]s are partially or completely self-closed by their nearest neighbors by means of multiple C-H···O interactions[29c] in solid state and then in this case, showed little interest for europium ions (Fig. S16†). Thus the CB[6]s in these frameworks are definitely not the main active sites, as Eu^{3+} ions only changed the PL spectra of **CB[6]HP** slightly (Fig. S30†).

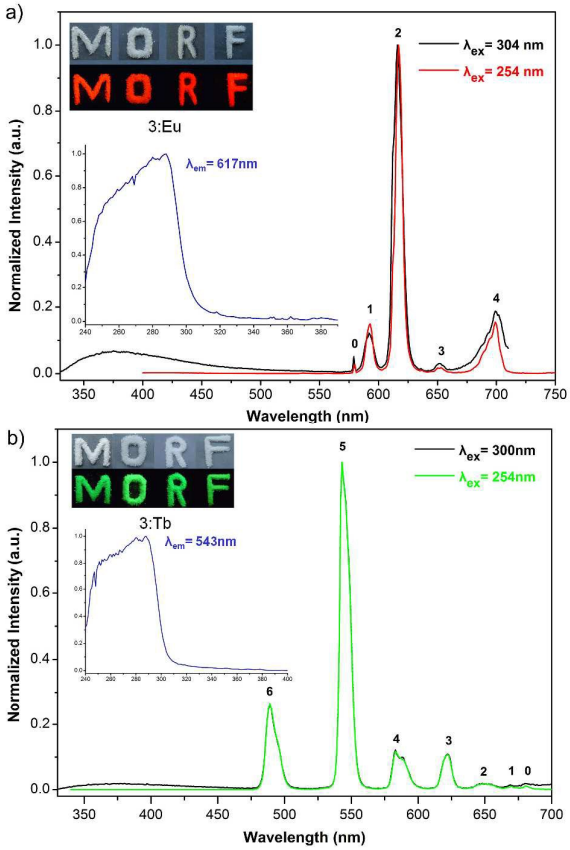

Fig. 9. Photoluminescence excitation (PLE) and emission spectra of a) **3:Eu** and b) **3:Tb** measured at room temperature. The insets are the optical photographs of 'MORF' written by corresponding composites, excited under 254 nm ultraviolet lamps. Emission bands 0-4 in a) correspond to transitions $^5D_0 \rightarrow {}^7F_J$, J = 0, 1, 2, 3, 4 (579, 593, 617, 652, 699 nm). Emission bands 6-0 in b) correspond to transitions $^5D_4 \rightarrow {}^7F_J$, J = 6, 5, 4, 3, 2, 1, 0 (489, 543, 583, 622, 648, 670, 680 nm). A broad PLE band at~280 nm corresponds to absorption of the *m*-BDC ligands[27e].

Encouraged by this, we chose **3** to prepare **3**:**Ln** (Ln= Sm^{3+}, Eu^{3+}, Tb^{3+} and Dy^{3+}), the PLE and UV/vis spectra of which further confirmed the coordination interactions (Fig. 9 and Fig. S31-S33†). Compared to that of **3**, it is noted that **3:Ln** showed similar significant adsorption bands before 300 nm, which were quite different from that of corresponding solid lanthanide nitrate (Fig. S34). This behaviour have been found in some Ln-based coordination polymers.[27e] Under excitation at 254 nm, the PL spectra of **3:Eu** displays series of emission peaks within 580-720 nm and they can be assigned to the $^5D_0 \rightarrow {}^7F_J$ (J =0, 1, 2, 3, 4) transitions of Eu^{3+}. The observation of the formally forbidden $^5D_0 \rightarrow {}^7F_0$ transition in the spectra of **3:Eu** suggests low local symmetry for Eu^{3+} ions on the surfaces of **3**. As for **3:Tb**, the strongest peak situated at 543 nm ascribed to $^5D_4 \rightarrow {}^7F_5$ transition is responsible for the green light emission of the composite.[27c] The maximum excitation wavelength was located at 280 nm. Their quantum yield were selectively measured at room temperature under the same conditions. A value of 21.3% was achieved for **3:Tb**, which was

much higher than that of **3:Eu** (2.2%). This is probably due to the better match of electronic band of ligands with the resonance level of Tb^{3+} ions than Eu^{3+} ions.[26a, 27e] Therefore, it is suggested that the coordination interactions between lanthanide ions and carboxylic groups of **3** contributed to the sensitization as the main factor.

Conclusions

In summary, the versatile mixed ligands strategy proved to be efficient for constructing five new metal-organic rotaxane frameworks (MORFs) by combining cucurbit[6]uril-based pseudorotaxanes ($[PR64]^{2+}$ or $[PR63]^{2+}$), rigid geometry varied carboxylate ligands (H_2BDC, H_2BPDC, *m*-H_2BDC or H_3BTC) and metal ions. The various architectures of compound **1**-**5** have shown that the topologies of resultant MORF could be tuned by both the geometry and length of auxiliary ligands and metal ions with different coordination numbers. Structural analysis revealed that non-covalent interactions around CB[6], such as hydrogen bonding, C–H···π and π···π interactions could affect the formation of resulted solid hybrids, like **1**, **2** and **3**. While in **4** and **5**, CB[6] or pseudorotaxane $[PR63]^{2+}$ did play a 'template' role for the resulted intriguing architectures. The high efficiency of mixed ligands approach here demonstrates the potential power of using CB[6]-based MIMs as building blocks to generate a diverse range of new MORFs. We are currently exploring other functional ligands with different geometries, length, changes and potential SBBs in order to construct functional porous MORFs.

Acknowledgements

This work was financially supported by the NSFC of China (No. 21471027, 21171033, 21131001, 21222105), National Key Basic Research Program of China (No. 2013CB834802), Changbai mountain scholars of Jilin Province and FangWu distinguished young scholar of NENU. We thank Prof. Jean-Claude Bünzli and Dr. Wei-Jin Li for their helpful suggestions.

Notes and references

1 (a) N. W. Ockwig, O. D. Friedeichs, M. O'Keeffe, O. M. Yaghi, *Acc. Chem. Res*. 2005, **38**,176-182; (*b*) O. M. Yaghi, M. O'Keeffe, N. W. Ockwig, H. K. Chae, M. Eddaoudi, J. Kim, *Nature.*, 2003, **423**, 705; (*c*) H. Furukawa, K. E. Cordov, M. O'Keeffe, O. M. Yaghi, *Science*. 2013, **341**, 1230444; (*d*) S. R. Batten, N. R. Champness, X. M. Chen, J. Garcia-Martinez, S. Kitagawa, L. Öhrström, M. O'Keeffe, M. P. Suh, and J. Reedijk, *Pure Appl. Chem.*, 2013, **85**, 1715–1724; (*e*) *2012 metal-organic frameworks issue*. *Chem. Rev*. 2012, **112**, 673; http://pubs.acs.org/toc/chreay/112/2.

2 For some recent reviews on mechanically interlocked molecules (MIMs) and their applications see: (*a*) *Molecular Catenanes, Rotaxanes and Knots: A Journey through the World of Molecular Topology*, ed. J.-P. Sauvage, C. Dietrich Buchecker, Wiley-VCH, Weinheim, 1999; (*b*) J. F. Stoddart, *Chem. Soc. Rev.*, 2009, **38**, 1802-1820; (*c*) H. X. Deng, M. A. Olson, J. F. Stoddart and O. M. Yaghi, *Nat. Chem.*, 2010, **2**, 439-443; (*d*) O. Lukin and F. Vögtle, *Angew. Chem. Int. Ed*. 2005, **44**, 1456-1477; (*e*) L. Fang, M. A. Olson, D. Benítez, E. Tkatchouk, W. A. Goddard III and J. F. Stoddart, *Chem. Soc. Rev.*, 2010, **39**, 17-29; (*f*) W. Yang, Y. Li, H. Liu, L. Chi, and Y. L. Li, *Small*., 2012, **8**, 504-516; (*g*) E. A. Neal and S. M. Goldup, *Chem. Commun*., 2014, **50**, 5128-5142.

3 (*a*) Q. Li, C. H. Sue, S Basu, A. K. Shveyd, W. Zhang, G. Barian, L. Fang, A. A. Sarjeant, J. F. Stoddart, and O. M. Yaghi, *Angew. Chem. Int. Ed*., 2010, **49**, 6751-6755; (*b*) A. Coskun, M. Hmadeh, G. Barin, F. Gándara, Q.W. Li, E. Choi N. L. Strutt, D. B. Cordes, A. M. Z. Slawin, J. F. Stoddart, J. P. Sauvage and O. M. Yaghi, *Angew. Chem. Int. Ed.* 2012, **51**, 2160；(*c*) V. N. Vukotic, K. J. Harris, K. L. Zhu, R. W. Schurko and S. J. Loeb, *Nature Chemistry*, 2012, **4**, 456-460; (*d*) K. Zhu, V. N. Vukotic, C. A. O'Keefe, R. W. Schurko, and S. J. Loeb, *J. Am. Chem. Soc*. 2014, **136**, 7403-7409; (*e*) K. L. Zhu, C. A. O'Keefe, V. N. Vukotic, R. W. Schurko, and S. J. Loeb, *Nature Chemistry*, 2015, DOI: 10.1038/NCHEM.2258.

4 (*a*) S. J. Loeb, *Chem. Commun.*, 2005, 1511-1518; (*b*) V. N. Vukotic and S. J. Loeb, *Chem. Soc. Rev*., 2012, **41**, 5896-5906; (*c*) J. Yang, J. F. Ma, and S. R. Batten, *Chem. Commun*., 2012, **48**, 7899-7912. The metal-organic rotaxane frameworks (MORFs) termed by Loeb should be distinguished from the polyrotaxane metal-organic frameworks (PMOFs) recently reviewed by Batten when topos analysis is applied. The main difference is that the former is based on predesigned pseudorotaxanes or rotaxanes, which usually contains host macro-molecule, while the later is largely dependent on in situ formed metal-ligand loops.

5 (*a*) K. Kim, N. Selvapalam, Y. H. Ko, K. M. Park, D. Kim and J. Kim, *Chem. Soc. Rev*., 2007, **36**, 267-279; (*b*) K. Kim, *Chem. Soc. Rev*., 2002, **31**, 96-107; (*c*) Y.-M. J. D. Whang, J. Heo, and K. Kim,, *J. Am. Chem. Soc.*,, 1996, **118**, 11333-11334; (*d*) E Lee, and K. Kim., *Angew. Chem. Int. Ed.*, 2000, **112**, 2811. (*e*) K.-M. Park, S,-Y. Kim, J. Heo, D. Whang, S. Sakamoto, K. Yamaguchi, and K. Kim, *J. Am. Chem. Soc*., 2002, **124**, 2140-2147; (*f*) J. –P. Zeng, H. Cong, K. Chen, S. -F. Xue, Y. –Q. Zhang, Q. J. Zhu, J. X. Liu and Z. Tao, *Inorg. Chem.*, 2011, **50**, 6521–6525; (*g*) J. Liang, X. -L. Wang, Y. -Q. Jiao, C. Qin, K. -Z. Shao, Z. -M. Su and Q. Y. Wu, *Chem. Commun*., 2013, **49**, 8555-8557; (*h*) L. Mei, Q. -Y. Wu, C. -M. Liu, Y. -L. Zhao, Z. -F. Chai and W. -Q. Shi, *Chem. Commun.*, 2014, **50**, 3612-3615; (*i*) K.-M. Park, D. Whang, E. Lee, J. Heo, K. Kim, *Chem.-Eur. J.* 2002, ***8***, 498; (j) X. S. Wu, J. Liang, X. L. Hu, X. L. Wang, B. Q. Song, Y. Q. Jiao, Z. M. Su, *Crystal Growth & Design*, 2015, **15**,4311-4317.

6 (*a*) D. J. Hoffart, S. J. Loeb, *Angew. Chem.,* 2005, **117**, 923 – 926; (*b*) L. K. Knight, V. N. Vukotic, E. Viljoen, C. B. Caputo and S. J. Loeb, *Chem Commun*, 2009, 5585-5587; (*c*) D. J. Mercer, V. N. Vukotic and S. J. Loeb, *Chem. Commun.,* 2011, **47**, 896–898; (*d*) V. N. Vukotic. S. J. Loeb, *Chem. Eur. J.*, 2010, **16**, 13630 – 13637; (*e*) N. C. Frank, D. J. Mercer and S. J. Loeb, *Chem. Eur. J.*, 2013, **19**, 14076-14080.

7 (*a*) H. Y. Gong, B. M. Rambo, E. Karnas, V. M. Lynch, K. M. Keller, and J. L. Sessler, J. Am. Chem. Soc. 2011, **133**, 1526–1533; (*b*) H. Y. Gong, B. M. Rambo, C. A. Nelson, V. M. Lynch, X. Zhu and J. L. Sessler, *Chem Commun.*, 2012, **48**, 10186-10188; (*c*) H.-Y. Gong, B. M. Rambo, W. Cho, V. M. Lynch, M. Oh and J. L. Sessler, *Chem. Commun.*, 2011, **47**, 5973.

8 (*a*) C. -F. Lee, D. A. Leigh, R. G. Pritchard, D. Schultz, S. J. Teat, G. A. Timco, R. E. P. Winpenny, *Nature*. 2009, **458**, 314-318; (*b*) C. -Y. Gao, L. Zhao, M.-X. Wang, *J. Am. Chem. Soc*., 2011, **133**, 8448-8451; (*c*) G. F. S. Whitehead, B. Cross, L. Carthy, V. A. Milway, H. Rath, A. Fernandez, S. L. Heath, C. A. Muryn, R. G. Pritchard, S. J. Teat, G. A. Timco and R. E. P. Winpenny, *Chem. Commun*., 2013, **49**, 7195-7197.

9 (*a*) Y. Liu, Y. L. Zhao, H. Y. Zhang and H. B. Song, *Angew. Chem., Int. Ed.*, 2003, **42**, 3260–3263; (*b*) L. Yu, M. Li, X. -P. Zhou, and D. Li, *Inorg. Chem*., 2013, **52**, 10232-10234.

10 *Organizing Mechanically Interlocked Molecules to Function Inside Metal-Organic Frameworks[M]/Molecular Machines and Motors*, K. -L. Zhu, S. J. Loeb, Springer, 2014: 213-251.
11 (*a*) J. W. Lee, S. Samal, N. Selvapalam, H.-J. Kim, and K. Kim, Acc. Chem. Res., 2003, **36**, 621-630; (*b*) J. Lagona, P. Mukhopadhyay, S. Chakrabarti, and L. Isaacs, *Angew. Chem. Int. Ed*., 2005, **44**, 4844-4870; (*c*) L. Isaacs, *Chem. Commun*., 2009, 619-629; (*d*) Y. Ahn, Y. Jang, N. Selvapalam, G. Yun, and K. Kim, *Angew. Chem. Int. Ed.*, 2013, **52**, 3140-3144; (*e*) K. -D. Zhang, J. Tian, D. Hanifi, Y. Zhang, A. C. -H. Sue, T. -Y. Zhou, L. Zhang, X. Zhao, Y. Liu and Z.-T. Li, J. *Am. Chem. Soc*., 2013, **135**, 17913-17918.
12 (*a*) X. -L. Ni, X. Xiao, H. Cong, L. -L. Liang, K. Cheng, X. J. Cheng, N. N. Ji, Q. -J. Zhu, S. -F. Xue and Z. Tao, *Chem. Soc. Rev*., 2013, **42**, 9480-9508; (*b*) J. Lü, J. -X. Lin, M.-N. Cao, R. Cao, *Coord. Chem. Rev*., 2013, **257**, 1334-56.
13 (*a*) S. Angelos, Y. W. Yang, K. Patel, J. F. Stoddart, and J. I. Zink, *Angew. Chem. Int. Ed*., 2008, **47**, 2222-2226; (*b*) W. S. Jeon, A. Y. Ziganshina, J. W. Lee, Y. H. Ko, J. K. Kang, C. Lee, and K. Kim, *Angew. Chem. Int. Ed.*, 2003, **115**, 4231-4234.
14 J. Zhang, , R. J. Coulston, S. T. Jones, J. Geng, O. A. Scherman, C. Abell, *Science*., 2012, **335**, 690-694.
15 (*a*) X. -L. Ni, X. Xiao, H. Cong, Q. -J. Zhu, S. -F. Xue, and Z. Tao, *Acc. Chem. Res*., 2014, **47**, 1386-1395; (*b*) K. Chen, Y.-S. Kang, Y. Zhao, J. -M. Yang, Y. Lu and W. -Y. Sun, *J. Am. Chem. Soc.*, 2014, **136**, 16744-16747.
16 K. –M. Park, S. -Y. Kim, J. Heo, D. Whang, S. Sakamoto, K. Yamaguchi, K. Kim, *J. Am. Chem. Soc.*, 2002, **124**, 2140-2147.
17 (*a*) O. K. Farha, K. L. Mulfort, A. M. Thorsness and J. T. Hupp, *J. Am. Chem. Soc.*, 2008, **130**, 8598-8599; (*b*) Y. S. Bae, K. L. Mulfort, H. Frost, P. Ryan, S. Punnathanam, L. J. Broadbelt, J. T. Hupp and R.Q. Snurr, *Langmuir*, 2008, **24**, 8592-8598; (*c*) S. Henke, A. Schneemann and R. A. Fischer, *Adv. Funct. Mater*., 2013, **23**, 5990-5996; (*d*) M. M. J. Smulders, I. A. Riddell, C. Browne and J. R. Nitschke, *Chem. Soc. Rev.*, 2013, **42**, 1728-1754.
18 (*a*) E. Lee, J. Kim, J. Heo, D. Whang and K. Kim, *Angew. Chem., Int. Ed.*, 2001, **40**, 399-402; (*b*) Y. Diskin-Posner, G. K. Patra and I. Goldberg, *Eur. J. Inorg. Chem*., 2001, 2515-2523; (*c*) L. K. Knight, V. N. Vukotic, E. Viljoen, C. B. Caputo, and S. J. Loeb, *Chem. Commun*., 2009, 5585-5587.
19 (*a*) Z.-B. Wang, H. -F. Zhu, M. Zhao, Y.-Z. Li, T. Okamura, W. -Y. Sun, H.-L. Chen, and N. Ueyama, *Crystal Growth & Design*., 2006, **6**, 1420-1427; (*b*) Z. B. Wang, M. Zhao, Y. Z. Li, H. –L. Chen, *Supramolecular Chemistry*, 2008, **20**, 689. Pseudorotaxanes $[PR6n]^{2+}.2[NO3]^{-}$ (n= 3, 4) was prepared by threading Cucurbit[6]uril with N,N -bis(n-pyridine)-1,6-diammoniumhexane dinitrate $[C6Nn]^{2+}.2[NO_3]^{-}$ in a 'slippage' way.
20 (*a*) T. Gadzikwa, O. K. Farha, K. L. Mulfort, J. T. Hupp and S. T. Nguyen, *Chem. Commun*., 2009, 3720-3722; (*b*) J. Cao, Y. Gao, Y. Wang, C.-F. Du and Z. -L. Liu, *Chem. Commun*., 2013, **49**, 6897-6899; (*c*) X. Meng, R. L. Zhong, X. Z. Song, S. Y. Song, Z. M. Hao, M. Zhu, S. N. Zhao and H. J. Zhang, *Chem. Commun*., 2014, **50**, 6406-6408.
21 (*a*) A. Harada, A. Hashidzume, H. Yamaguchi and Y. Takashima, *Chem. Rev*., 2009, **109**, 5974-6023; (*b*) D. Ajami and J. Rebek, Acc. Chem. Res., 2012, **46**, 990-999; (c) T. Ogoshi and T. Yamagishi, *Chem. Commun.*, 2014, **50**, 4776-4787.
22 (*a*) V. A. Blatov, *IUCr CompComm. Newsletter*., 2006, **7**, 4-38; see also http://www.topos.ssu.samara.ru; (*b*) DIAMOND 3.2, CRYSTAL IMPACT, Postfach 1251, Bonn, 2009; (*c*) A. L. Spek, *PLATON, A multipurpose crystallographic tool*, Utrecht. University, The Netherlands, 2003.
23 L. Carlucci, G. Ciani, D. M. Proserpio, *Coord. Chem. Rev.*, 2003, **246**, 247-289.
24 To the best of our knowledge, **4** represents the first *snw* MORFs in coordination polymers, as the other three cases were based on hydrogen bonds between small organic molecules.[22a]
25 (*a*) J. W. Lee, Y. H. Ko, S.-H. Park, K. Yamaguchi and K. Kim, *Angew. Chem., Int. Ed.*, 2001, **40**, 746-749; (*b*) L. Xu, L. J. Chen and H. B. Yang, *Chem. Comm*., 2014, **50**, 5156-5170.
26 (*a*) Y. J. Cui, Y. F. Yue, G. Qian, B. L. Chen, *Chem. Rev*. 2012, **112**, 1126-1162; (*b*) H. -D. Guo, X. -M. Guo, S. R. Batten, J. -F. Song, S.-Y. Song, S. Tang, G. L. Zheng, J. -K. Tang, H.-J. Zhang, *Crystal Growth & Design*, 2009, **9**, 1394-1401; (*c*) B. Tram, N. Pham, L. M. Lund, D. Song, *Inorg. Chem*., 2008, **47**, 6329-6335; (*d*) Y. Qiu, Y. Li, G. Peng, J. Cai, L. Jin, L. Ma, H. Deng, M. Zeller, S. R. Batten, *Crystal Growth & Design,* 2010, **10**,1332-1340.
27 (*a*) O. A. Gerasko, E. A. Mainicheva, M. I. Naumova, O. P. Yurjeva, A. Alberola, C. Vicent, R. Llusar, and V. P. Fedin, *Eur. J. Inorg. Chem.*, 2008, 416-424; (*b*) O. A. Gerasko, E. A. Mainicheva, M. I. Naumova, M. Neumaier, M. M. Kappes, S. Lebedkin, D. Fenske, and V. P. Fedin, *Inorg. Chem*., 2008, **47**, 8869-8880; (*c)* F. F. da Silva, C. A. F. de Oliveira, E. H. L. Falcão, J. Chojnacki, J. L. Neves, S. A. Jr, *Dalton Trans*., 2014, **43**, 5435-5442; (*d*) R. Decadt, K. V. Hecke, D. Depla, K. Leus, D. Weinberger, I. V. Driessche, P. V. D. Voort and R. V. Deun, *Inorg. Chem*., 2012, **51**, 11623-11634; (*e*) H. Zhang, L. Zhou, J. Wei, Z. Li, P. Lin and S. Du, *J. Mater. Chem*., 2012, **22**, 21210-21217.
28 Fresh long hexagonal prism CB[6] (CB[6]HP) crystals were prepared to make composites CB[6]HP:Eu. We observed that hexagonal CB[6] *P6/mmm* crystals[29c] with perfectly aligned one dimensional macrocycle nanotubes couldn't retain its original crystallinity after being soaked in ethanol for a few days (Fig. S16†).
29 (*a*) D. Bardelang, K. A. Udachin, D. M. Leek, and J. A. Ripmeester, *CrystEngComm*., 2007, **9**, 973-975; (*b*) S. Lim, H. Kim, N. Selvapalam, K. J. Kim, S. J. Cho, G. Seo, and K. Kim, *Angew. Chem., Int. Ed.*, 2008, **120**, 3400-3403; (*c*) D. Bardelang, K. A. Udachin, D. M. Leek, J. C. Margeson, G. Chan, C. I. Ratcliffe, and J. A. Ripmeester, *Crystal Growth & Design*, 2011, **11**, 5598-5614.

Syntheses, crystal structures and properties of metal-organic rotaxane frameworks with cucurbit[6]uril

Jun Liang,[a,b] Xue-Song Wu,[a] Xin-Long Wang,[*a] Chao Qin,[a] Kui-Zhan Shao,[a] Zhong-Min Su,[*a] and Rong Cao[b]

Received (in XXX, XXX) Xth XXXXXXXXX 20XX, Accepted Xth XXXXXXXXX 20XX

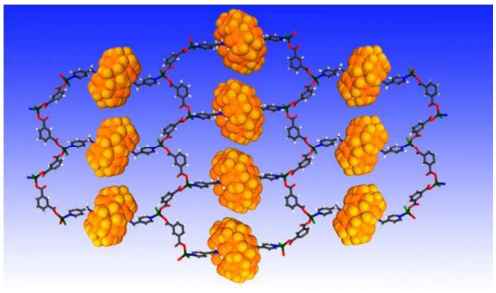

Five new cucurbit[6]uril-based MORFs are hydrothermally synthesized by the mixed ligands strategy and their fluorescence properties have been investigated.